Electronic Supplementary Material (ESI) for PCCP

Supporting Information for

Nanoparticle Dispersion in Polymer Nanocomposites by Spin-Diffusion-Averaged Paramagnetic Enhanced NMR Relaxometry: Scaling Relations and Applications

Bo Xu,[*a] *Johannes Leisen*[b] *and Haskell W. Beckham*[*a]

[a]*School of Materials Science and Engineering, Georgia Institute of Technology, 801 Ferst Drive, Atlanta, GA 30332 USA. E-mail: bxu6@gatech.edu; beckham@gatech.edu*

[b]*School of Chemistry and Biochemistry, Georgia Institute of Technology, 901 Atlantic Drive, Atlanta, GA 30332 USA*

This file contains:

*Corresponding authors. E-mail: bxu6@gatech.edu; beckham@gatech.edu

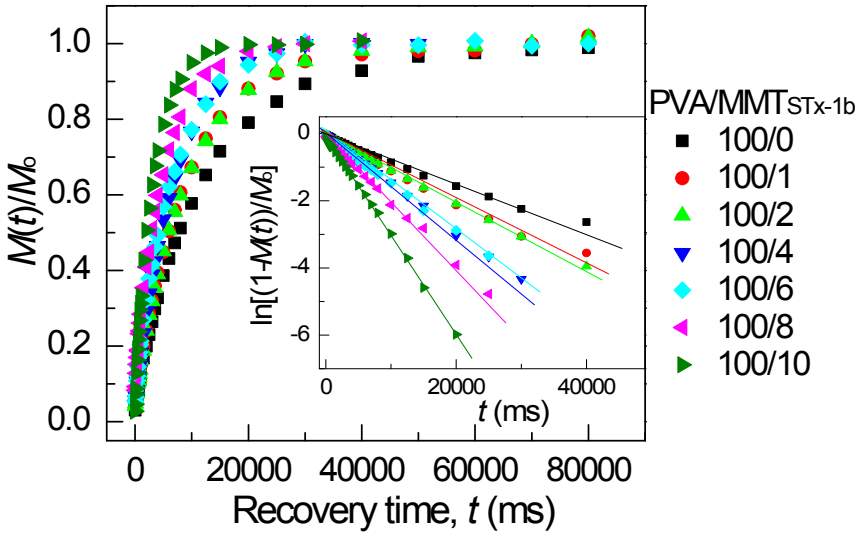

Figure S1. Normalized magnetization, $M(t)/M_o$, versus recovery time, t for pure poly(vinyl alcohol) and poly(vinyl alcohol)/montmorillonite (PVA/$MMT_{STx\text{-}1b}$) nanocomposites at weight ratios (PVA/$MMT_{STx\text{-}1b}$) of 100/1, 100/2, 100/4, 100/6, 100/8, and 100/10. The inset displays the same data plotted as $\ln[1 - M(t)/M_o]$ versus recovery time, t, the slopes of which reflect the inverse T_1s. The relaxation rate increases upon increasing the $MMT_{STx\text{-}1b}$ content; all nanocomposites exhibit faster relaxation (shorter T_1^H) than the corresponding pure PVA. The calculated T_1 values are 11.64 ± 0.23 s, 9.38 ± 0.23 s, 9.21 ± 0.11 s, 7.01 ± 0.0.07 s, 6.67 ± 0.12 s, 5.00 ± 0.11 s and 3.10 ±0.23 s for weight ratios from 100/0 to 100/10, respectively.

Model analysis: sinks with infinitely fast relaxation

As discussed in the main text, we recently reported an analytical relationship between NMR magnetization growth and interparticle spacings (IPS) in lamellar polymer/paramagnetic clay nanocomposites:[1]

$$\frac{M(t)}{M_o} = 1 - \left(\frac{4D}{\beta\Delta^2}\right)^{1/2} \tan\left(\frac{\beta\Delta^2}{4D}\right)^{1/2} \exp(-t/T_{1,s}) - \frac{8}{\pi^2}\sum_{n=0}^{\infty}\frac{1}{(2n+1)^2}\left[\frac{1}{1-(2n+1)^2\pi^2 D/(\beta\Delta^2)}\right]\exp\left[-\left(\frac{(2n+1)^2\pi^2 D}{\Delta^2}+\frac{1}{T_{1,m}}\right)t\right] \quad (5)$$

where M_0 is the total equilibrium magnetization, D is the bulk spin diffusion coefficient (uniform, not a function of spatial position), $1/T_{1,m}$ is the bulk matrix nuclear relaxation rate, $1/T_{1,s}$ is the relaxation rate of the clay surface nuclei, and β is the difference between $1/T_{1,s}$ and $1/T_{1,m}$ (i.e., $\beta = 1/T_{1,s} - 1/T_{1,m}$). In the case of the sinks with infinitely fast relaxation (e.g., $T_{1,s} \rightarrow 0$, i.e., $\beta \rightarrow \infty$), we can simplify eq 5:

$$\frac{M(t)}{M_o} = 1 - \sum_{n=0}^{\infty} \beta_n^{-1} \exp\left[-\left(\frac{8\beta_n D}{\Delta^2} + \frac{1}{T_{1,m}} \right) t \right] \tag{S1}$$

where $\beta_n = (2n + 1)^2\pi^2/8$. The summation in eq S1 converges quite rapidly with n; numerical calculation using just two iterations yields errors less than 5% (see Figure S2). Taking only the first term of the summation, equation S1 can be recast:

$$\frac{M(t)}{M_o} = 1 - \frac{8}{\pi^2} f(t) \exp\left[-\left(\frac{\pi^2 D}{\Delta^2} + \frac{1}{T_{1,m}} \right) t \right] \tag{S2}$$

where $f(t) = 1 + 1/9 \exp(-8B\ t) + 1/25 \exp(-24B\ t) + \ldots$, and $B = \pi^2 D/\Delta^2$. The value of $f(t)$ approaches 1 if $t > (8B)^{-1} = 8\Delta^2/(\pi^2 D)$. Note that this approximation is valid when spin diffusion lengths, $(D \times 5T_1)^{1/2}$, are greater than interparticle separations, Δ. In other words, the interparticle distance is such that magnetization throughout the entire sample may equilibrate due to spin diffusion during the T_1 relaxation process. Thus, samples must be characterized by $T_1 > \Delta^2/(20D)$. Since this is approximately $(8B)^{-1} = 8\Delta^2/(\pi^2 D)$, eq S2 should sufficiently describe long-time relaxation behavior for $f(t) = 1$ (i.e., $n = 0$ in summation of eq S1). This was

confirmed by numerically generating relaxation curves for the first four n values of the summation (n = 0, 1, 2 and 3) using parameter values similar to those for a PCN with 5 wt% MMT and a spin diffusion coefficient, D = 0.7 nm^2/ms. These are shown in Figure S2(a) and reveal no difference in the long-time relaxation behavior when t > ~180 ms ≈ $8\Delta^2/(\pi^2 D)$. Although differences are observed in the short-time behavior, Figure S2(b) shows that these do not significantly affect the overall T_1 values determined from plots of $\ln[\pi^2/8(1-M(t)/M_o)]$ versus recovery time. As a result, from eq S2 with $f(t)$ = 1, the observed $1/T_{1,PCN}$ can be obtained

$$\frac{1}{T_{1,PCN}} \approx \frac{\pi^2 D}{\Delta^2} + \frac{1}{T_{1,m}} \tag{S3}$$

Equation S3 can be compared to the semi-empirical equation used to compute the paramagnetic contribution to the spin-lattice relaxation rate:[2-4]

$$R_{1,para} = 1/T_{1,para} = 1/T_{1,PCN} - 1/T_{1,polymer} \tag{S4}$$

if the relaxation rate of the pure polymer, $1/T_{1,polymer}$, is taken to be the relaxation rate of the bulk polymer in the nanocomposite, $1/T_{1,m}$. In this case, the paramagnetic contribution to the relaxation is

$$R_{1,para} \approx \pi^2 D/\Delta^2 \tag{S5}$$

Thus, $R_{1,para} \sim \Delta^{-2}$, for sinks with infinitely fast relaxation (*e.g.*, $T_{1,s} \rightarrow 0$, *i.e.*, $\beta \rightarrow \infty$).

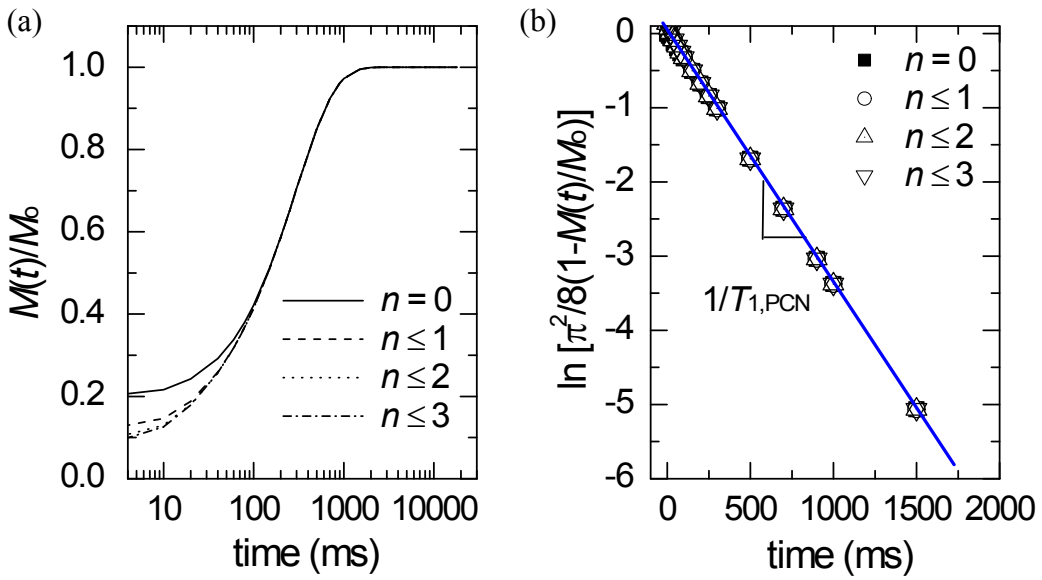

Figure S2. Relaxation curves numerically calculated using eq S1 and the first four terms of $f(t)$, corresponding to eq S2 (first term of summation only) and $n = 0$, ≤ 1, ≤ 2 and ≤ 3: (a) $M(t)/M_o$, and (b) $\ln[\pi^2/8(1 - M(t)/M_0)]$ versus recovery time. The following parameters were used in the calculation: spin diffusion coefficient, $D = 0.7$ nm^2/ms, bulk polymer relaxation time, $T_{1,m} = 1.635$ s, $\Delta = 50$ nm and recovery time range from 0.5 to 10000 ms. Calculated values of $T_{1,\,PCN}$ in (b), 296 ms ($n = 0$), 293 ms ($n \leq 1$), and 292 ms (n ≤ 2 and ≤ 3), are consistent with the relaxation constant of 296 ms determined by fitting the data points in (b) to a conventional exponential recovery.

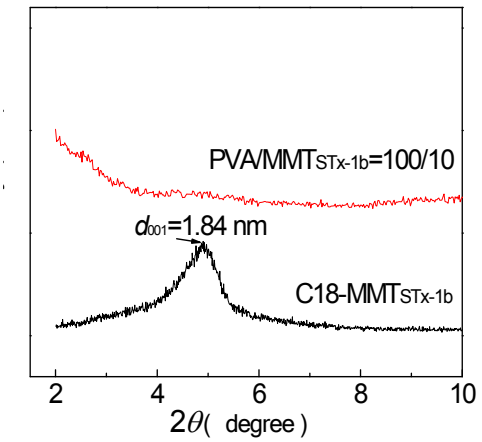

Figure S3. X-ray diffraction patterns of octadecylamine-modified $MMT_{STx\text{-}1b}$ (C18-$MMT_{STx\text{-}1b}$) and a PVA/$MMT_{STx\text{-}1b}$ nanocomposite (PVA/$MMT_{STx\text{-}1b}$ = 100/10, w/w). This PVA/$MMT_{STx\text{-}1b}$ nanocomposite contains 10 wt% clay and does not exhibit a basal peak (001) reflection, indicating the clay is exfoliated.

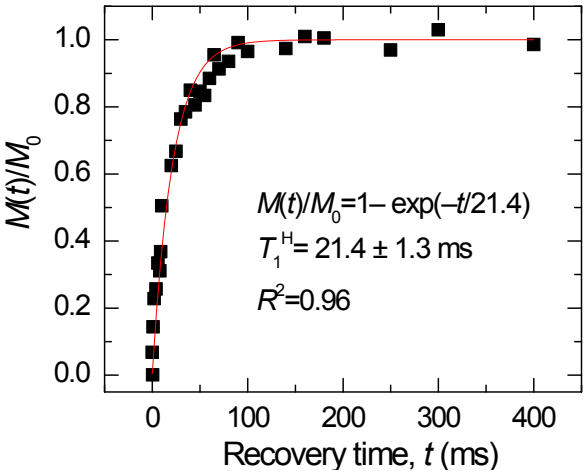

Figure S4. Normalized magnetization, $M(t)/M_o$ versus recovery time for octadecylamine-modified $MMT_{STx\text{-}1b}$ (C18-$MMT_{STx\text{-}1b}$) measured at 300 MHz. T_1^H = 21.4 ± 1.3 ms.

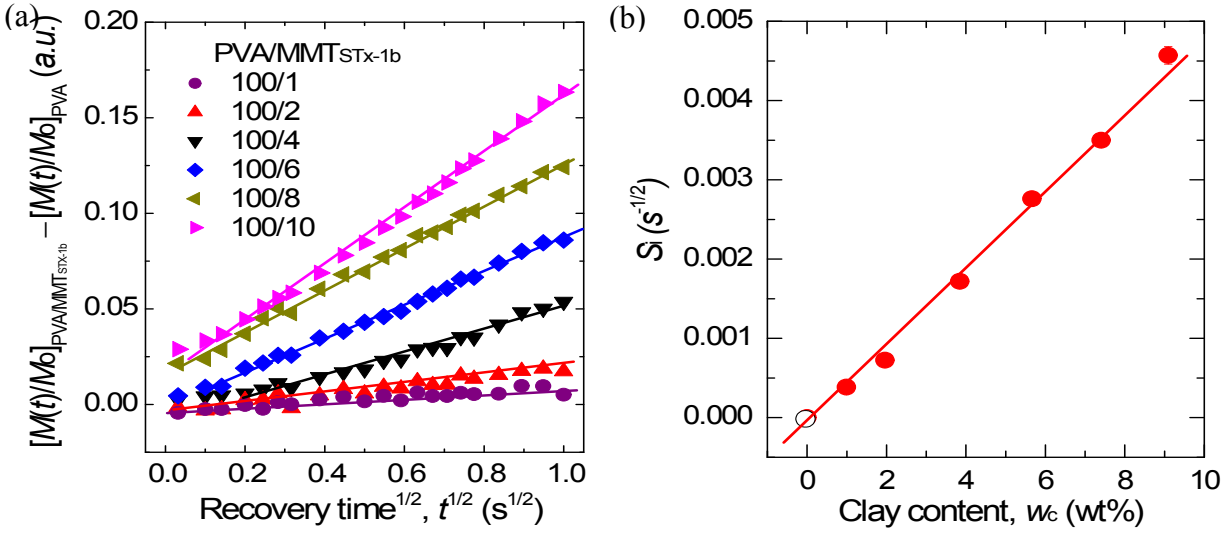

Figure S5. (a) Normalized and corrected magnetization versus the square root of recovery time for poly(vinyl alcohol)/montmorillonite ($PVA/MMT_{STx\text{-}1b}$) nanocomposites with different clay contents. $PVA/MMT_{STx\text{-}1b}$ weight ratios are 100/x where x = 1, 2, 4, 6, 8 and 10. The data were measured at 300 MHz and are vertically displaced to prevent overlap. Lines are linear least-square fits. Slopes of these lines, S_i are plotted in (b) as a function of clay content, w_c. These initial slopes, which reflect the effective clay/polymer interfacial area, are linearly proportional to the clay weight fraction and therefore suggest similar degrees of exfoliation in these samples.

References

(1) Xu, B.; Leisen, J.; Beckham, H. W. Nanoparticle dispersion in polymer nanocomposites by spin-diffusion-averaged paramagnetic enhanced NMR relaxometry. *Nanoscale* **2014**, *6*, 1318–1322.

(2) Xu, B.; Leisen, J.; Beckham, H. W.; Abu-Zurayk, R.; Harkin-Jones, E.; McNally, T. Evolution of Clay Morphology in Polypropylene/Montmorillonite Nanocomposites upon Equibiaxial Stretching: A Solid-State NMR and TEM Approach. *Macromolecules* **2009**, *42*, 8959-8968.

(3) Bertmer, M.; Wang, M. F.; Kruger, M.; Blumich, B.; Litvinov, V. M.; van Es, M. Structural changes from the pure components to nylon 6-montmorillonite nanocomposites observed by solid-state NMR. *Chemistry of Materials* **2007**, *19*, 1089-1097.

(4) Calberg, C.; Jerome, R.; Grandjean, J. Solid-state NMR study of poly(epsilon-caprolactone)/clay nanocomposites. *Langmuir* **2004**, *20*, 2039-2041.